

R. L. Bruhn*
W. T. Parry
M. P. Bunds

Department of Geology and Geophysics, University of Utah, Salt Lake City, Utah 84112, USA

ABSTRACT

Faulting controls fluid migration within transpressive fault-propagation folds in the Cook Inlet forearc basin of south-central Alaska. Na-Ca-Cl brine migrates out of Mesozoic rocks through reverse and oblique-slip faults into the cores of anticlines, where the fluid spreads laterally outward into lower Tertiary strata by flow through cross faults and permeable beds. Precipitation of zeolite and carbonate cement and veins reduces the permeability of folded bedding and faults. Zeolite minerals are formed by chemical reactions between Na-Ca-Cl brine and sedimentary rocks. Carbonate minerals are precipitated when Na-HCO₃ connate fluid in the Tertiary section reacts with rocks during diagenesis, and by mixing of migrated Na-Ca-Cl brine with the Na-HCO₃ pore fluid. Carbonate cement is also precipitated by fluctuations in PCO₂ during faulting and jointing.

High fluid pressure is encountered while drilling through lower Tertiary and Mesozoic strata in some anticlines. High-pressure fluid is contained within porous beds that are intercalated with strata cemented by carbonate and zeolite minerals. Zeolite and carbonate cemented beds retard the dissipation of high fluid pressure, and channel fluid flow parallel to bedding within the anticlines. High fluid pressure may be generated by several processes, acting either alone or together. The evidence for fault-controlled migration of fluid out of the basement suggests that volumetric strain related to deformation is most important, but may be augmented by dynamo-thermal metamorphism, sedimentary compaction, alteration of organic-rich rock and hydrocarbons, and possibly glacial loading.

*E-mail: rlbuhn@mines.utah.edu.

Keywords: fluid pressure, forearc basins, petroleum geology, structural geology, tectonics.

INTRODUCTION

Fluid pressures significantly above or below hydrostatic occur in a variety of tectonic settings, from stable regions to actively deforming plate margins (Ortoleva et al., 1995; Powley, 1990; Hunt, 1990). Abnormal pressure is found in compartments bounded by low-permeability rocks that inhibit pressure equilibration between adjacent regions. Clay-rich strata are most often cited as potential seals (Deming, 1994), but recent studies have proposed that seals may also be formed by diagenetic and hydrothermal minerals (Ortoleva et al., 1995).

The goals of this study are to determine the distribution of fluid pressure, to determine the origin of cement and vein minerals that inhibit fluid flow, and to evaluate mechanisms for fluid migration and fluid-pressure generation within the upper, or northeastern, part of Cook Inlet basin (Fig. 1). Active tectonics, together with extensive subsurface data collected during more than 30 years of hydrocarbon exploration and production, make the basin an attractive natural laboratory for studying the interplay between geodynamics, fluid-pressure generation, fluid migration, and diagenesis. Some previous studies conclude that high-pressure fluid is trapped by calcite-cemented seals, which cut across stratigraphic boundaries in oil field anticlines and occupy steeply dipping faults (Powley, 1990; Hunt, 1990). Alternatively, others conclude that there is little evidence for anomalous fluid pressure in seal-bounded compartments (Franks and He-Zhiyong, 1995). A resolution to this problem is important for several reasons. Migration of hydrocarbons is partly controlled by the spatial and temporal distribution of fluid pressure, but information on the fluid pressure regime has not been integrated into published petroleum system

models (Kirschner and Lyon, 1973; Magoc 1994). Faults in Cook Inlet basin may generate damaging earthquakes in the most populated and industrialized part of Alaska (Detterman et al. 1974; Haeussler, in press). Studying spatial variations in fluid pressure may help to identify mechanically unstable faults, with high potential for earthquake generation. If calcite seals cut across stratigraphy and structure (Powley, 1990; Hunt, 1990), then fault decollement may be controlled by the thermodynamics of mineral dissolution and precipitation rather than by mechanical anisotropy imparted by sedimentary layering.

RESEARCH METHODS

Research work included making observations and collecting samples from outcrops and drill cores; compiling and analyzing well log, fluid pressure, and rock permeability measurements; analyzing geochemistry of cement and vein minerals; and geochemical modeling of chemical reactions among basin fluids and rocks. ARCO Alaska Inc. provided access to seismic reflection data that were used to construct geologic cross sections of selected anticlines. Construction of the cross sections and interpretations relevant to earthquake generation were discussed in detail by Haeussler et al. (in press). In this study we focus on the relationship between faulting, folding, and fluid migration.

TECTONICS OF UPPER COOK INLET BASIN

Cook Inlet is located in a forearc basin bounded by the Chugach and Kenai Mountains to the southeast, and the Alaska Range and Aleutian volcanic arc to the northwest (Fig. 1; Dickinson and Seeley, 1979). The geodynamics of Cook Inlet basin are complex because of the protracted history of deformation associated with subduction and microplate collision (Plafker et al., 1994). Regional transpression is caused by mechanical cou-

pling between the North American and Pacific plates, and collision of the Yakutat block at the eastern end of the subduction zone. The depth to the subducting Pacific plate is 50–60 km beneath the basin's center and deeper on its northwest side (Page et al., 1991).

Large faults bound three of the basin's margins: the Castle Mountain fault at the northeast end of the basin, the Bruin Bay fault in the foothills of the Alaska Range, and the Border Ranges fault along the northern flanks of the Chugach and Kenai Mountains (Fig. 2; Grantz, 1966; Pavlis, 1982; Plafker et al., 1994). Paleozoic and Mesozoic rocks in the Alaska Range are part of an accreted arc and microcontinent that collided with North America during Cretaceous time (Silberling et al., 1994). These rocks extend southeastward beneath Cook Inlet basin and outcrop as fault-bounded slivers and klippen along the flanks of the Chugach and Kenai Mountains. Mesozoic sedimentary rocks in the Chugach and Kenai Mountains are part of a vast accreted complex that was faulted against and thrust beneath the southern edge of the continental margin. Tertiary strata in Cook Inlet basin are therefore deposited on a polyglot basement of Paleozoic and Mesozoic metamorphic and igneous rocks, and Jurassic through Cretaceous marine strata.

Cook Inlet basin formed as Paleocene streams deposited strata over deformed Mesozoic and older rocks (Fig. 3; Calderwood and Fackler, 1972). Lower Tertiary strata and volcanic rocks were deformed by regional strike-slip faulting and folding during Eocene and early Oligocene time (Barnes and Payne, 1956; Clardy, 1974; Stamatakis et al., 1988, 1989; Little, 1991). Transpression formed a complex structural terrain of folds, faults, eroded horst blocks, and adjacent grabens filled with synorogenic fluvial deposits. Conglomerate and coarse sandstone were deposited over much of the basin as deformation waned, forming the Hemlock, Bell Island, and Tsadaka Formations (Calderwood and Fackler, 1972; Clardy, 1974). Deposition of lower Miocene fluvial strata buried this middle Tertiary structural terrain prior to the onset of late Miocene to Holocene deformation (Kirschner and Lyon, 1973; Calderwood and Fackler, 1972). Neogene deformation continued along parts of the Bruin Bay and Castle Mountains faults, and initiated fault-propagation folding throughout the basin (Fig. 4; Kirschner and Lyon, 1973; Boss et al., 1976). The anticlines contain prolific oil and gas reservoirs (Kirschner and Lyon, 1973; Magoon, 1994).

The anticlines are cored by reverse to oblique-slip faults that root in the Mesozoic and older basement rocks and cut upward through lower and middle Tertiary strata (Fig. 4; Kirschner and Lyon, 1973; Haeussler et al., in press). The anticlines are also cut by numerous cross faults that

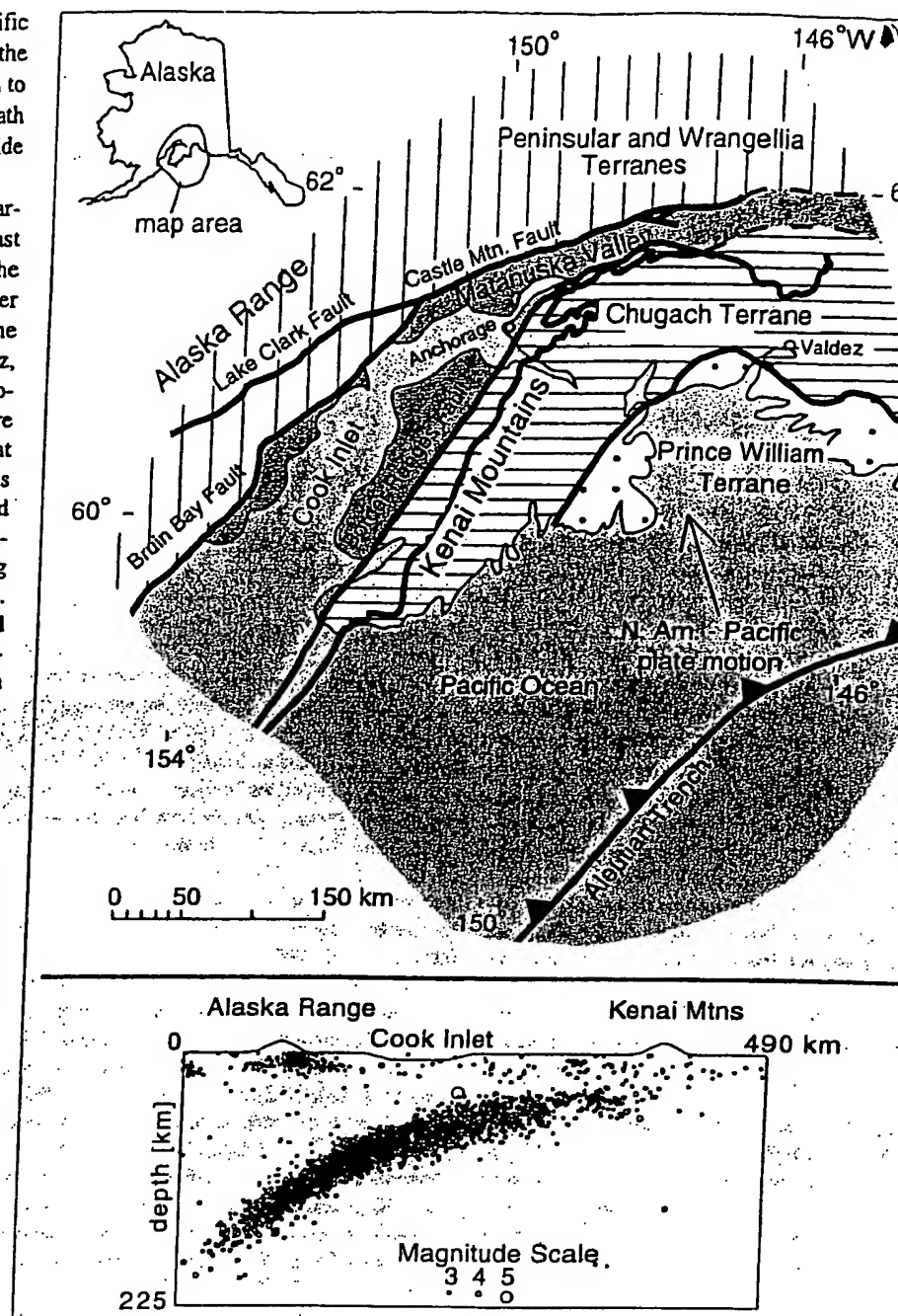


Figure 1. Tectonic map of the southern Alaskan plate margin showing the location of Cook Inlet Basin. The cross section shows the distribution of earthquakes in the Benioff zone North American plate in the Cook Inlet region for a 10 yr period. Earthquakes are projected onto a west-northwest–east-southeast vertical plane. Earthquake data provided by John L. U.S. Geological Survey seismicity catalog.

offset fold hinges, and subdivide oil and gas fields into distinct hydrologic units (Alaska Oil and Gas Conservation Commission, 1994). Kirschner and Lyon (1973) proposed that displacement on cross faults was mostly normal slip, but both outcrop exposures and structural contours of cross-faulted folds indicate predominantly strike-slip displacement (Fig. 4A; Barnes and Payne, 1956; Bruhn

and Pavlis, 1981; Alaska Oil and Gas Conservation Commission, 1994).

Carbonate and zeolite veins and cement occur in both large reverse-slip faults and smaller cross faults where observed in lower Tertiary and older strata (Fig. 5). The veins formed during multiple episodes of fluid flow and deformation. Evidence for mineral precipitation during faulting includes

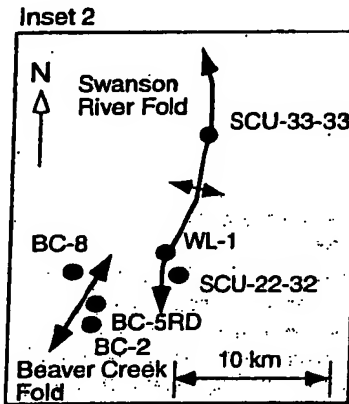
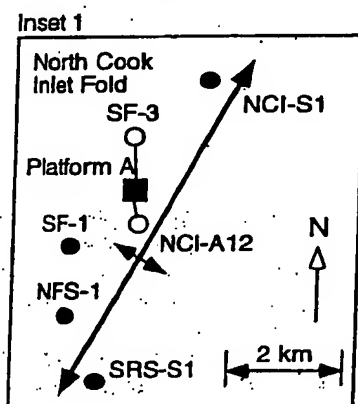
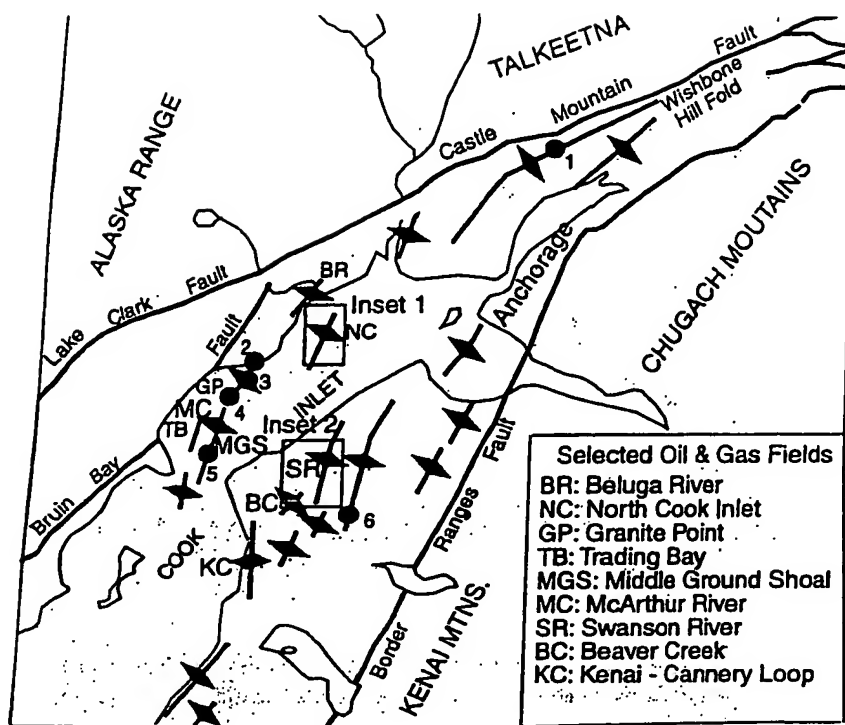


Figure 2. Tectonic map of upper Cook Inlet showing large faults, prominent anticlines and oil and gas fields. Insets 1 and 2 enclose North Cook Inlet and Swanson River anticlines. Numbers indicate locations of wells listed in Table 1.

multiple sets of crosscutting veins, and mineral fibers elongated parallel to fault striae in both drill core and outcrop. Faults in late Miocene and younger rocks are discrete zones of cataclasis and gouge with few vein minerals.

The distribution of fluid pressure within Cook Inlet basin must be considered in context of the history of hydrocarbon generation, migration, and trapping. Reservoirs in the upper Miocene Beluga Formation and Pliocene Sterling Formation produce gas generated by biogenic alteration of coal beds (Claypool et al., 1980). Oil and gas produced from the lower Miocene Tyonek Formation and older strata are primarily derived from thermal maturation of organic-rich, marine source beds in the Middle Jurassic Tuxedni Group (Magoon and Claypool, 1981). Hydrocarbon migration oc-

curred in two phases, according to Magoon and Claypool (1981) and Magoon (1994). Hydrocarbons first migrated into traps along the angular unconformity between Mesozoic and lower Tertiary rocks. These traps were breached by deformation and erosion during middle Tertiary time. Deposition of Miocene strata was followed by renewed migration during late Miocene to Holocene faulting and folding. Hydrocarbons became trapped in the crests of growing anticlines during this latest phase of migration.

LITHOLOGY OF TERTIARY AND UPPER MESOZOIC SEDIMENTARY ROCKS

Tertiary strata are sandstone, conglomerate, siltstone, and coal deposited in meandering and

Calderwood and Fackler, 1972). These dep are as much as 9 km thick in the deepest pa Cook Inlet basin, but Miocene and youi strata thin over the crests of anticlines bec of erosion and stratal offlap caused by folk (Kirschner and Lyon, 1973; Boss et al., 15 Haeussler et al., in press). Detrital grains are intermediate composition volcanic, metamorp and plutonic lithic fragments, and quartz, i gioclase, and less common K-feldspar, deri from erosion of the surrounding mountai Middle to upper Mesozoic strata are mos lithicwacke, siltstone, mudstone, shale, a minor limestone deposited in a marine envirc ment over a Jurassic arc and older basemei However, fluvial strata and coal beds also occ in Upper Cretaceous deposits (Magoon et a 1980).

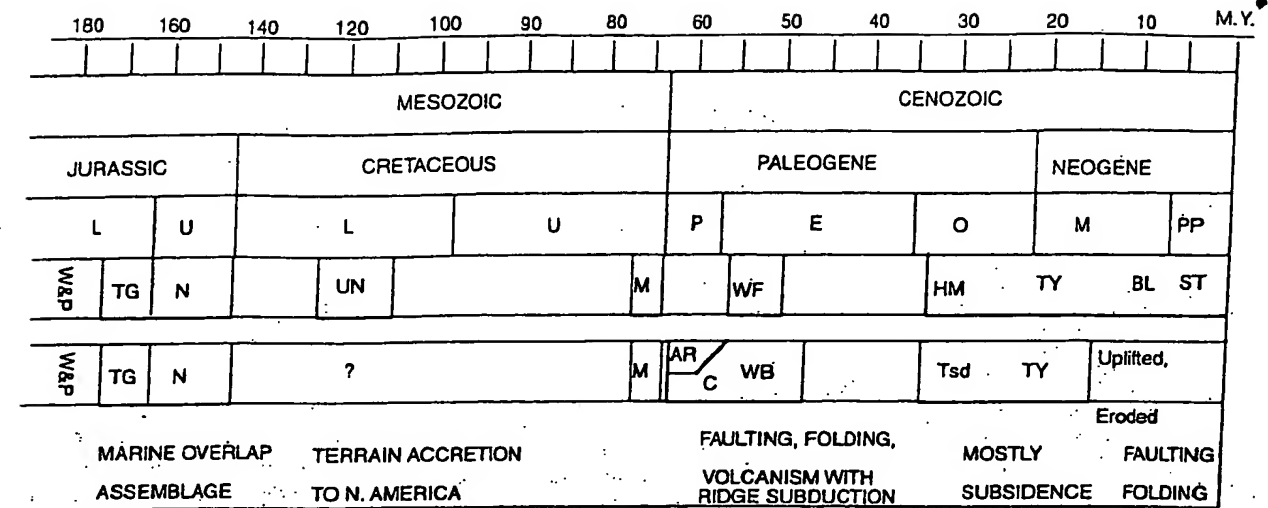
Cement and vein minerals decrease the porosi and permeability of sedimentary rocks and fault forming aquitards to fluid flow. Cement minera include clay, quartz, chlorite, calcite, siderite dolomite, and zeolites (Hayes, 1979; Lyle an Morehouse, 1977; Fisher and Magoon, 1978). Secondary carbonate and zeolite cements are abundant in lower Miocene and older sedimentary rocks, where calcite and siderite fill pores and replace original feldspar grains, clay, chlorite, and quartz. Laumontite and prehnite, as well as carbonate minerals, seal fractures and cement pores in the Paleocene West Foreland Formation and older rocks throughout much of the basin.

The carbonate- and zeolite-cemented rocks form low-permeability, lenticular stringers and tabular beds intercalated between more porous and permeable beds from which cement and framework grains were partly dissolved. The lateral dimensions of secondary cemented and secondary porosity-enhanced beds could not be established between wells. However, siderite and calcite-cemented sandstone and conglomerate beds, meters to tens of meters thick, extend for tens to hundreds of meters along strike in the mining high wall of Paleocene coal measures in the Wishbone Hill fold in the Matanuska Valley (Fig. 5). This exhumed fold is structurally analogous to folds in the subsurface of upper Cook Inlet basin.

FLUID-PRESSURE MEASUREMENTS

Methods

Information on fluid pressure was compiled from published summaries of initial reservoir production pressure (Alaska Oil and Gas Conservation Commission, 1994), from drill stem test (DST) and repeat formation test (RFT) records, and by interpretation of well log petrophysics measurements obtained from reports and files of the Alaska Oil and Gas Conservation Commis-



FORMATION NAMES & SYMBOLS

ST: Sterling Fm.
 BL: Beluga Fm.
 TY: Tyonek Fm.
 HM: Hemlock Fm.
 WF: West Foreland Fm.
 M: Matanuska Fm.
 UN: Unnamed Rocks.
 N: Naknek Fm.
 TG: Tuxedni Group
 W&P: Wrangellia & Peninsula Terranes

Tsd: Tsadaka Fm., also Bell Island Sandstone
 WB: Wishbone Hill Fm.
 C: Chickaloon Fm.
 AR: Arkose Ridge Fm.

Figure 3. Stratigraphy with annotated tectonic history of upper Cook basin (upper column) and the adjacent Matanuska Valley (lower column) (see Fig. 2).

sion. We selected pressure records from exploration wells after determining that reported pressures were not in error because of leaking packers or other problems during testing (Table 1).

Initial Reservoir Pressure. Initial fluid pressures in Cook Inlet gas and oil reservoirs were tabulated and published by the Alaska Oil and Gas Conservation Commission (1994; Fig. 6A). Initial pressures generally increase systematically with reservoir depth at a rate of ~10–11 MPa/km (Fig. 6A). Initial pressure is between 10% and 20% above hydrostatic in several shallow gas reservoirs in the Beluga, Sterling, and Tyonek Formations, and in oil reservoirs in the Hemlock Conglomerate in the Swanson River oil field. Few production reservoirs are located below a depth of 3 km, the proposed transition depth from normal to high fluid pressure in the basin proposed by Hunt (1990). Evidence for fluid pressure at greater depth must be gleaned from fluid-pressure measurements and petrophysics logs collected in exploration wells.

Fluid-Pressure Measurements. DST and RFT results from exploration wells are listed in Table 1 and plotted with respect to depth in Figure 6B. Several aspects of these fluid pressure measurements are noteworthy.

1. Fluid pressure is mostly hydrostatic above 3 km depth, but becomes greater than hydro-

static in some deeper intervals, as discussed by Hunt (1990).

2. Fluid pressure fluctuates with depth rather than increasing monotonically along either hydrostatic or abnormally high pressure gradients. Consider the Sunfish #3 exploration well in the North Cook Inlet anticline (Fig. 2; Table 1), for example. Fluid pressure in the Tyonek Formation is hydrostatic until the C-sands are encountered at 3400 m, where fluid pressure is 50 MPa, or 33% greater than hydrostatic (Fig. 6B; Table 1). Fluid pressure beneath the C-sands decreases to 43 MPa, or nearly hydrostatic pressure at 3750 m (Table 1).

3. Fluid pressure varies between wells in the same stratigraphic interval. For example, fluid pressure in the lower Tyonek Formation C-sands is significantly different in the Sunfish #1 and #3 wells, which both penetrate the North Cook Inlet anticline (Fig. 2; Table 1). Fluid pressure in the C-sands is approximately hydrostatic in the Sunfish #1 well, but is 33% above hydrostatic in the Sunfish #3 well located ~10 km to the north in the same anticline.

4. Fluid pressure is greater than hydrostatic in Mesozoic rocks in the Swanson River anticline. High fluid pressure was measured in the Upper Cretaceous Matanuska Formation and the Upper Jurassic Naknek Formation (Table 1).

Petrophysics Measurements. Sonic velocity logs provide additional evidence for the distribution of overpressure in the core of the Swanson River anticline, where DSTs in high fluid pressure in Mesozoic rocks (Tyonek wells SCU-33-33 and SCU-22-32). The transit time (ITT) of compressional waves traveling through rocks next to the well bore decreases with depth because porosity is reduced by compaction, causing sonic velocity to increase (Serra, 1986). However, rocks with high fluid pressure are undercompacted. Undercompaction results in lower compressional wave velocity and increased ITT. This is illustrated by the velocity log in the SCU-33-33 well (Fig. 6C) where we have plotted ITT in sandstone. The ITT decreases systematically along a roughly linear trend on the semilogarithmic plot, depth of ~4000 m. Below ~4000 m the ITT fluctuates about a nearly vertical trend in undercompacted sandstone beds that are intercalated with mudstone and shale. We interpret this velocity anomaly to be caused by overpressure in Mesozoic sandstone in the core of the fold.

PERMEABILITY MEASUREMENTS

Permeability measurements are compiled from well test and commercial laboratory reports.

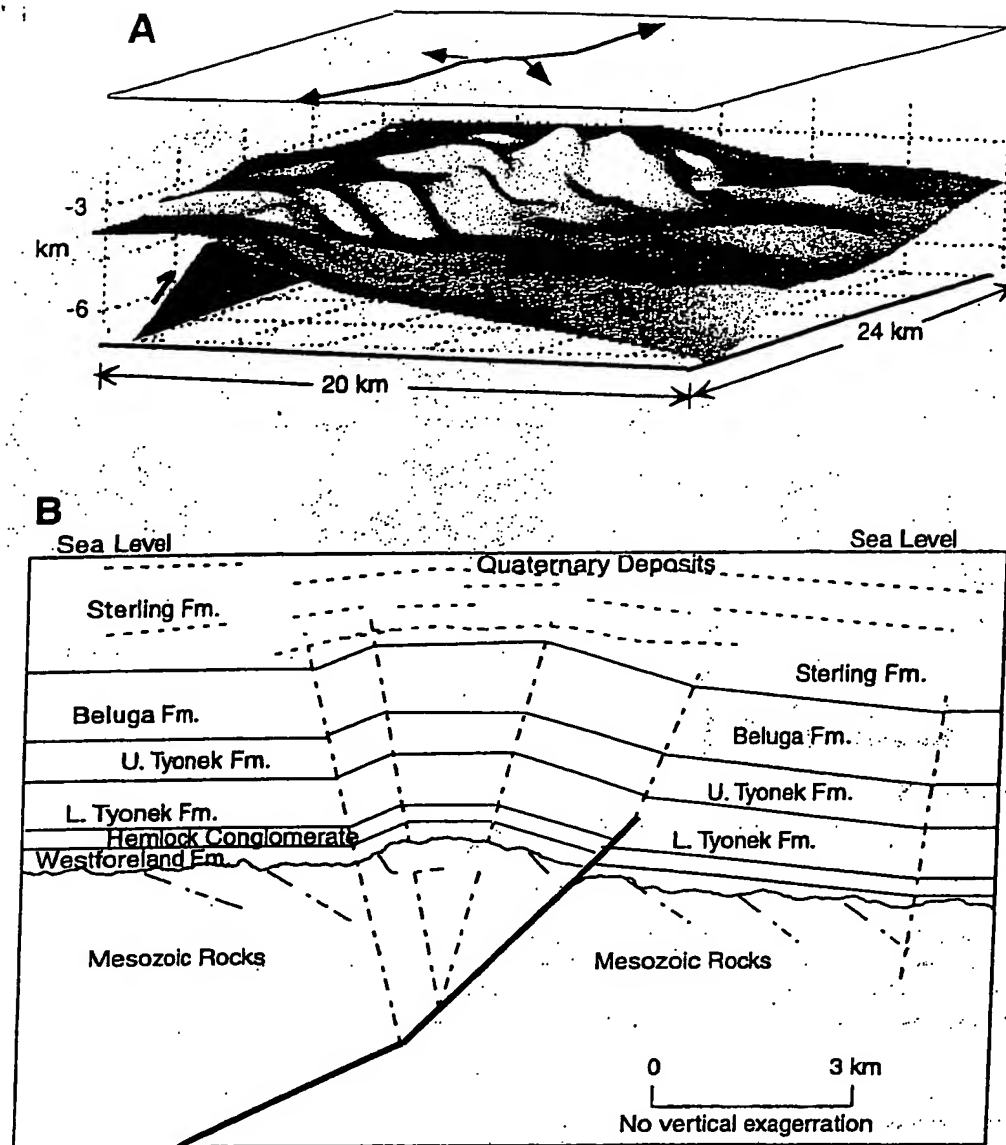


Figure 4. (A) Structural configuration of Hemlock conglomerate in the Swanson River anticline constructed from structural contour maps prepared by oil field operators and exploration companies. Lateral and vertical offsets of the fold crest are caused by cross faulting, perhaps like that in the Wishbone Hill fold (Fig. 5). (B) Geologic cross section of the North Cook Inlet anticline showing reverse or oblique-reverse faults in the core of the anticline.

on file with the Alaska Oil and Gas Conservation Commission. The permeability measurements are mostly from sandstone and siltstone in potential reservoir strata, rather than lower permeability mudstone and shale. The equipment used by commercial laboratories also restricts measurements of low-permeability rocks. The lower permeability limit for most commercial laboratory tests was $\sim 10^{-17} \text{ m}^2$, with the exception of core samples from the Sun Fish #3 well, where the instrument detection limit was $\sim 10^{-18} \text{ m}^2$. Only a few tests are made at elevated confining pressure; most are air-permeability tests at atmospheric pressure. Here we discuss core plug measure-

ments from the Sun Fish #3 well in the North Cook Inlet anticline. Several Tertiary and Mesozoic formations were tested in this well; some of the tests were done at elevated confining pressure, and in several intervals core plugs were drilled both parallel and normal to bedding.

Permeability is reported for strata in the Mesozoic Naknek and Matanuska Formations, and the overlying West Foreland, Hemlock Conglomerate, and Tyonek Formations in the Sunfish #3 well. Permeability (k) spans several orders of magnitude, ranging from the lower detection limit of $k \approx 10^{-18} \text{ m}^2$ to a high of $k \approx 10^{-13} \text{ m}^2$ in the most permeable samples. Permeability measured

greater than perpendicular to bedding. Coarse grained rocks are more permeable than fine grained rocks, with the exception of intervals of secondary carbonate and zeolite cement. In the latter intervals, the permeability of conglomerate and sandstone decreases markedly, and in some cores conglomerates are almost as impermeable or even more so, than adjacent siltstone, creating alternating bands of higher and lower permeability that mimics vertical variations in bedding. The vertical distribution of secondary cement fluctuates markedly between adjacent beds, and even within the same bed. This variability is detected either by visual inspection of the core, or by noting that the average grain density varies inversely with permeability because of high-density calcite and siderite cement (Fig. 8).

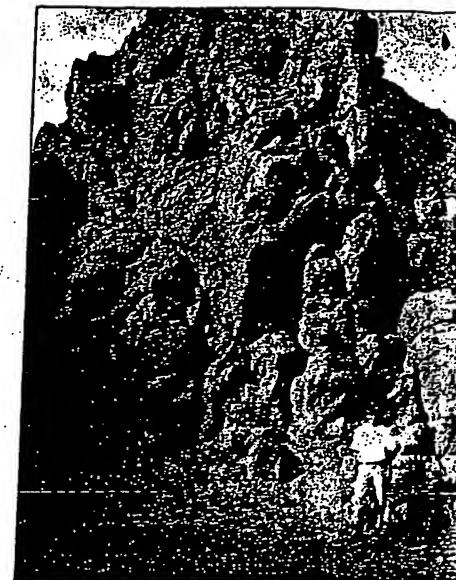
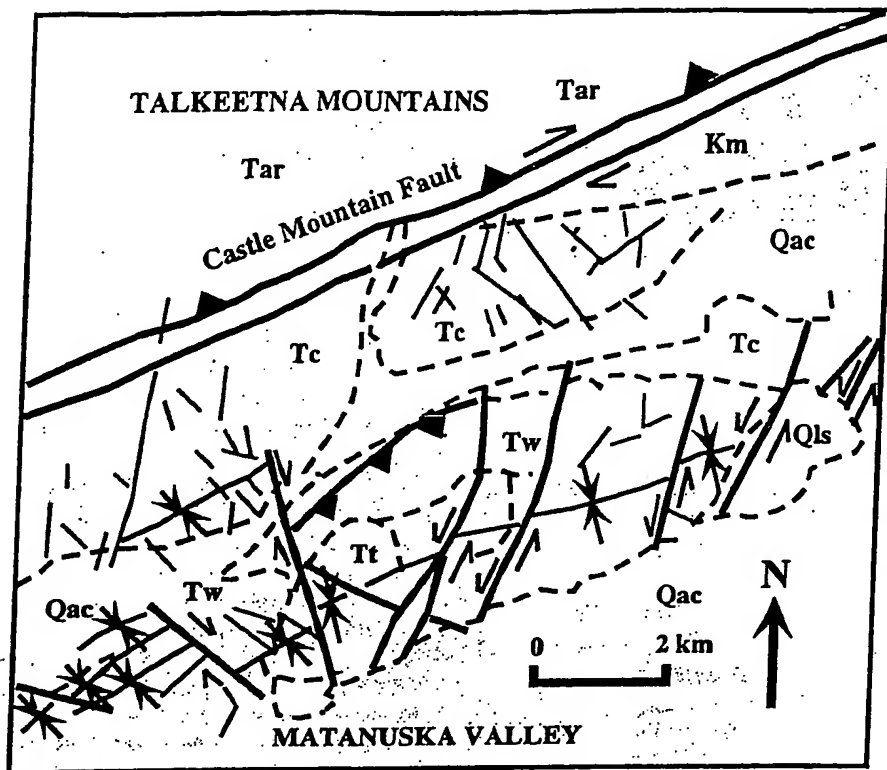
The permeability of packed off intervals several meters to tens of meters long was determined as part of DSTs and RFTs in several wells. The permeability ranges from $k < 10^{-18} \text{ m}^2$ in carbonate cemented intervals to much greater permeability in less cemented sandstone and conglomerate ($k = 10^{-14} \text{ m}^2$ to 10^{-12} m^2). For example, $k \leq 10^{-18} \text{ m}^2$ in lower Tyonek Formation sandstone and siltstone in the Big Lake #1 exploration well southeast of the Castle Mountain fault zone even though the formation has been uplifted several kilometers by folding and faulting.

FLUID COMPOSITION IN MESOZOIC AND TERTIARY ROCKS

Two chemically distinct pore fluids are present in Cook Inlet basin below a shallow fresh- to brackish-water transition (Table 2; McGee, 1977; Franks and He-Zhiyang, 1995). Oil and wet gas in lower Tertiary strata are associated with a Na-Ca-Cl brine containing 17 000 ppm to 35 000 ppm dissolved solids and relatively heavy $\delta^{18}\text{O}$ and δD . This fluid is altered seawater derived from Mesozoic marine source beds during diagenesis, and produces high-conductivity anomalies around the crests of some anticlines (McGee, 1977). Dry gas in late Miocene and younger reservoir rock is associated with an Na-HCO_3 brine with 3500–17 000 ppm, but typically between 3500 and 5000 ppm, total dissolved solids and lighter $\delta^{18}\text{O}$ and δD than the Na-Ca-Cl brine. This fluid is derived by alteration of fresh water trapped and buried in the Tertiary strata (Franks and He-Zhiyang, 1995).

STABLE ISOTOPE COMPOSITION OF CALCITE CEMENT AND VEINS

Carbon and oxygen isotopes were measured in calcite cement and veins in samples of Mesozoic and Tertiary rocks collected from drill cores. Veins were also collected from strike-slip



- Fault - arrows indicate strike-slip movement on upthrown side
- Photo-lineament (Fault?)
- Formation Contact
- Fold Axial Trace (syncline)

Figure 5. Geologic map of the Wishbone Hill fold, Matanuska Valley (Fig. 2). Resistant ridge of calcite and siderite veins and cement on the Eska fault, a left-lateral cross-fault that offsets Paleocene and Eocene strata in the Wishbone Hill fold. Qac—Quaternary glacial and deposits; Qls—Quaternary landslide; Tar—Arkose Ridge Formation (Paleocene); Tc—Chickaloon Formation (Paleocene–Eocene); Tw—Wishbone Hill Formation (Eocene); Tt—Tsadaka Formation (Oligocene); and Km—Matanuska Formation (Upper Cretaceous).

faults in the Wishbone Hill fold and Castle Mountain fault zone in the Matanuska Valley (Figs. 2 and 5). The samples show varying depletion of $\delta^{13}\text{C}$ from about 0‰ to -25‰ relative to Peedee belemnite (Fig. 9). Depletion of $\delta^{13}\text{C}$ below -5‰ is presumably caused by the influence of an organic carbon component.

There are three distinct trends in the $\delta^{18}\text{O}$ data (Fig. 9). Cements from Tertiary rocks are relatively light, cements from Mesozoic rocks are relatively heavy, and veins from faults are intermediate in oxygen isotopic composition. The $\delta^{18}\text{O}$ values of calcite cements presumably reflect isotopic equilibration between connate waters present in the rocks at about 80 °C. Fractionation between calcite and water at 80 °C is 19.5‰; thus the +20‰ values for Mesozoic cements represent equilibration between calcite and water with $\delta^{18}\text{O} = 0$ ‰, and +6‰ calcite in Tertiary rocks equilibrated with -13.5‰ water. Several calcite cement samples from lower Tertiary strata have intermediate and heavy $\delta^{18}\text{O}$, presumably due to either brine mixing or equili-

bration of the rock with fluid that migrated upward from the Mesozoic basement. The isotopic compositions of these inferred fluids match those of the Na-Ca-Cl and Na-HCO₃ fluids sampled in oil wells (Table 2). Intermediate $\delta^{18}\text{O}$ values in cement and veins could result from either mixing of these two fluids, or by fluid-rock reactions. The efficacy of these processes was investigated by geochemical modeling.

GEOCHEMICAL MODELING OF ZEOLITE AND CARBONATE PRECIPITATION

Precipitation of secondary calcite and zeolite cement and vein minerals reduced the permeability of lower Tertiary and older strata, and reverse- and strike-slip faults. Zeolite and carbonate cement may have precipitated during mixing of Na-Ca-Cl and Na-HCO₃ fluids, by reactions between these fluids and minerals in the rocks, and by changes in the partial pressure of CO₂ in pore fluid. These processes were modeled with

the speciation and reaction path program SOLVEQ and CHILLER (Reed, 1982). Temperature was fixed at 80 °C in all simulations, equivalent to the temperature at a depth between 1 and 4 km in upper Cook Inlet. Starting compositions of the two fluids were chosen with measured range of Na-Ca-Cl and Na-brines (Franks and He-Zhiyong, 1995; Tal-

Mixing Na-Ca-Cl brine with Na-HCO₃ precipitated both calcite and siderite (Fig. 9). Example results are cited for reference: mixing 1 kg of Na-Ca-Cl brine with 1.0 kg of Na-HCO₃ brine produced 1.6 g of calcite or 0.59 cm³ calcite per 1.5 kg of water. A total of 2.5×10^5 kg water, or 255 m³, is required to fill the pore volume in 1 m³ of rock with an initial porosity of

Chemical reactions of Na-Ca-Cl and Na-HCO₃ fluids with a sandstone consisting of 50% quartz, 40% plagioclase (An₄₂), 5% K-feldspar, chlorite, and 2% muscovite were also simulated. The simulations were carried to albite saturation although plagioclase continued to react. Muscovite, quartz, calcite, prehnite, laumontite,

Well Name	Reference #	Depth		Pressure		Formation
		(ft)	(m)	(Psi)	(MPa)	
Sunfish 1 (SF1)	Inset 1	9562	2898	4295	30	Tyonek
		10423	3158	4778	33	Tyonek
		10856	3290	5188	36	Tyonek
		10860	3291	5208	36	Tyonek
		12234	3707	6263	43	Tyonek
Sunfish 3 (SF3)	Inset 1	11253	3410	7200	50	Tyonek
		12303	3728	6276	43	Tyonek
N. Cook Inlet St. (NCI1)	Inset 1	4033	1222	1691	12	Sterling
		11015	3338	7579	52	Tyonek
SRS State 1 (SRS1)	Inset 1	15040	4558	12893	89	Tyonek
		16050	4864	13494	93	W. Foreland
Big Lake Test 1	1	4553	1380	2602	18	Bell Island
		5538	1678	3187	22	Tyonek
Naptowne Unit 24-8	6	6064	1838	2545	18	Sterling
		6333	1919	2648	18	Sterling
		6444	1953	2738	19	Beluga
		9421	2855	4775	33	Tyonek
		9445	2862	4798	33	Tyonek
SCU-22-32	Inset 2	14100	4273	9120	63	Naknek
SCU-33-33	Inset 2	13,500	4091	8000	55	Matanuska
Wolf Lake 1 (WL 1)	Inset 2	13373	4052	8000	55	Naknek
Beaver Cr. 5RD (BC5RD)	Inset 2	14953	4531	9250	64	Tyonek
Beaver Cr. 2 (BC 2)	Inset 2	14900	4515	7135	49	Hemlock
		15130	4585	6959	48	Hemlock
Beaver Cr. 8 (BC 8)	Inset 2	9233	2798	4600	32	Tyonek
		9248	2802	4432	31	Tyonek
Granite Point #1	3	8665	2628	4304	30	Tyonek
		9230	2797	4348	30	Tyonek
		11000	3333	7055	49	Hemlock (?)
MGS 17595	N.A.	5540	1679	2683	18	N.A.
		5942	1801	2687	19	N.A.
		6053	1834	2775	19	N.A.
		6079	1842	2803	19	N.A.
		7105	2153	3735	26	N.A.
		7700	2333	3785	26	N.A.
		8100	2455	3870	27	N.A.
		8400	2545	3745	26	N.A.
		8633	2616	4285	30	N.A.
MGS 18745	4	8835	2677	4095	28	N.A.
		10400	3152	4268	29	N.A.
Tyonek St. 18742	2	8270	2508	4025	28	Tyonek
W. Foreland 1	N.A.	9338	2829	4475	31	Tyonek

Note: N.A.—not available. Map reference refers to well location on either main map or inset maps in Figure 1.

chlorite were precipitated by reaction of the Na-Ca-Cl brine with sandstone (Fig. 10B). The fluid reached saturation with calcite after reaction with 0.3 g of rock, with chlorite after reaction with 0.8 g of rock, with prehnite after reaction with 1 g of rock, and with laumontite after reaction with 2.9 g of rock. Reaction with 4 g of rock precipitated 0.05 g of calcite. One m³ of rock with 10% porosity required 120 m³ of water to completely fill pore space with reaction products.

Quartz, muscovite, calcite, chlorite, and kaolinite were precipitated in simulated reactions of rock with Na-HCO₃ water (Fig. 10C). Reaction of water with 4 g of rock precipitated 0.25 g of calcite, and 1 m³ of rock required 136 m³ of Na-HCO₃ water to fill 10% porosity with reaction products.

Calcite precipitation was also simulated by decreasing the partial pressure of CO₂, a process that presumably occurs during fracturing. De-

creasing CO₂ pressure from 10 bar to 1 bar precipitated 0.025 cm³ of calcite per 1 kg of water. Complete sealing of 1 m³ of rock with 10% porosity required precipitation of calcite from 4000 m³ of water. Clearly, fluid mixing and fluid reaction with rock are more effective at sealing porosity than CO₂ loss.

GENERATION OF ABNORMAL FLUID PRESSURE

The temporal scale for decay of abnormal fluid pressure in a seal-bounded reservoir is a function of both the permeability and the thickness of the seal (Derning, 1994). Fluid pressure begins to decay in 10⁵ yr or less if the sealing interval is ≤1 km thick with permeability $k \geq 10^{-18}$ m² (e.g., Derning, 1994; Neuzil, 1995). This implies that mechanisms that generate high fluid pressure are either

ability of Mesozoic and Tertiary rocks in up-Cook Inlet basin. We group candidate mechanisms into several categories for discussion: (1) volumetric strain, (2) hydrocarbon generation and alteration, and (3) mineral dehydration. Several additional processes are eliminated from consideration because of the environment in Cook Inlet basin. Aquathermal pressuring is unlikely given the geothermal gradient of 20–25 °C/km (Osborne and Swarbrick, 1997). Petrographic observations indicate little porosity and permeability reduction to pressure solution. Topography-driven flow from mountains surrounding the basin was numerically modeled and rejected as a source of abnormal fluid pressure by He-Zhiyong and Franks (1995). Osmotic processes are also unlikely to generate high fluid pressure because shale beds are discontinuous in the Tertiary section.

The one-dimensional hydrodynamic disequilibrium equation proposed by Neuzil (1995) is used to estimate the efficacy of several alternative processes for generating abnormal fluid pressure

$$\Gamma \geq K/L \quad (1)$$

Γ is hydrodynamic or geologic forcing in units of s⁻¹, K is the hydraulic conductivity of either the reservoir or the reservoir bounding seal, and L is the half-width of the reservoir as measured across its smallest dimension. Permeability magnitude $k = 10^{-7} K$ for brine-filled pore space. High fluid pressure may be maintained indefinitely if inequality 1 is satisfied, otherwise reservoir pressure decays toward ambient pressure in the surrounding region (Neuzil, 1995).

Γ is either calculated, or discussed qualitatively, depending on available information concerning a specific mechanism. We conclude that abnormal fluid pressure may be maintained in reservoirs several kilometers or more in size if $\Gamma \geq 10^{-14}$ s⁻¹, given that 10^{-18} m² ≤ $k \leq 10^{-16}$ m² for most intervals of zeolite- and carbonate-cemented rock in Cook Inlet basin (Table 3). Presumably, the permeability of deformed and cemented shale and mudstone layers is <10⁻¹⁸ m², but these rocks were not tested for permeability. Shale and mudstone permeated by zeolite and carbonate cement and veins is more common in the Mesozoic section than in the lower Tertiary rocks.

Process Category 1: Volumetric Strain—Sedimentary Compaction, Tectonic Strain, and Glacial Loading

Volumetric strain alters fluid pressure and induces fluid flow because pore space either contracts or dilates.

Sedimentary Compaction. High fluid pressure may be generated by compaction and thermal expansion of pore fluid during subsidence and

burial (Bredehoeft and Hanshaw, 1968). Pliocene and Quaternary deposits thicken in synclines and thin over the crests of anticlines in upper Cook Inlet basin. Average sedimentation rates are estimated by sampling the Pliocene (Sterling Formation) and Quaternary deposit isopach map of Hartman et al. (1972) at 10 km intervals on a square grid, and then dividing the sedimentary thickness at each grid point by an elapsed time of 5.3 m.y. Sedimentation rates range from nearly zero along the crest of the Middle Ground Shoal anticline to $\approx 6 \times 10^{-4}$ m/yr in the deepest synclinal trough, with the average rate $dL/dt = 3 \times 10^{-4}$ m/yr. These rates are approximate because the base of the Pliocene Sterling Formation is difficult to detect in some well logs, and the base of the Sterling Formation may not mark the Miocene-Pliocene temporal boundary at all localities (S. Franks, 1997, personal commun.).

Hydrodynamic disequilibrium by sedimentary compaction is estimated (Neuzil, 1995):

$$\Gamma = -\left[\frac{(1+\nu)/3(1-\nu)}{\zeta_m \gamma_g + \zeta_t G} \right] dL/dt \quad (2)$$

where G = geothermal gradient (20 – 25 °C/km), $\zeta_m = 1 \times 10^{-8}$ Pa $^{-1}$, $\zeta_t = 10^{-4}$ C $^{-1}$, Poisson's ratio $\nu = 0.25$, $\gamma_g = 2.3 \times 10^4$ kg m $^{-2}$ s $^{-2}$ (specific weight of fluid saturated rock), and dL/dt = sedimentation rate (m/yr).

Setting an upper bound thermal gradient $G = 25$ °C/km and $dL/dt = 6 \times 10^{-4}$ m/yr in equation 2 yields $\Gamma \leq 4 \times 10^{-15}$ s $^{-1}$ (Table 3).

Tectonic Strain. Anomalous fluid pressure may be generated by volumetric strain during faulting and folding (Neuzil, 1995). We consider three different tectonic mechanisms: distributed deformation, tectonic compaction by shearing in fault zones (Blanpied et al., 1992), and poroelastic deformation (Scholz, 1990). Consider the case where deformation is distributed evenly across the basin, with a regional shortening rate of ~ 1 cm/yr, or $\sim 20\%$ of the plate convergence velocity. The linear strain rate $\epsilon_L = -3 \times 10^{-15}$ s $^{-1}$. Following Neuzil (1995), we set volumetric strain rate $\epsilon_v = 0.1 \epsilon_L$ and calculate:

$$\Gamma = |-\zeta \epsilon_v|, \quad (3)$$

where $\zeta = 0.1$ is the coefficient relating bulk volumetric strain to porosity loss (Neuzil, 1995), and $\Gamma = 3 \times 10^{-17}$ s $^{-1}$, two orders of magnitude less than forcing by sedimentary compaction.

Tectonic compaction and consolidation of fine-grained fault rocks decreases both porosity and permeability, traps fluid, and creates high pore pressure (Sibson, 1990; Sleep and Blanpied, 1992; Byerlee, 1993). The high pore pressure may trigger rupturing and release high-pressure fluid that flows vertically upward and laterally outward from the fault zone (Sibson, 1990; Blanpied et al., 1992; Byerlee, 1993).

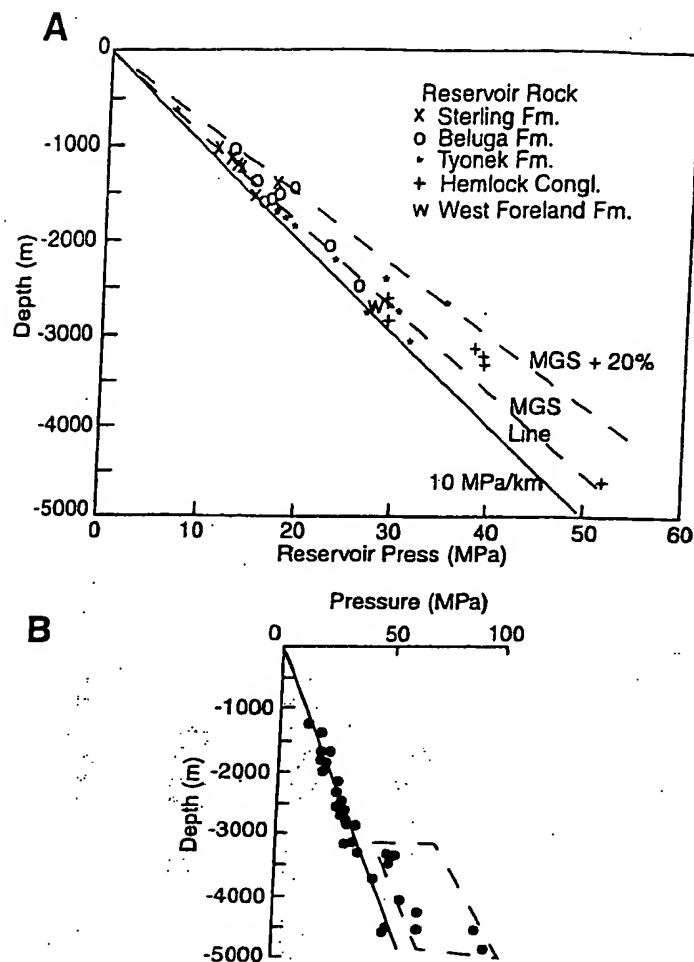


Figure 6. (A) Initial reservoir pressure versus reservoir depth. Solid lines denote hydrostatic pressure gradient for water, estimated hydrostatic gradient for brines in Middle Ground oil and gas field, and a reference line for fluid pressure gradient that is 20% in excess of Middle Ground Shoal gradient (MGS). Fluid pressure data are from AOGCC (1994). Middle Ground Shoal pressure gradients are from drill stem tests on file with Alaska Oil and Gas Conservation Commission. (B) Fluid pressure determined by drill stem and repeat formation in Cook Inlet exploration and production wells (see Table 1 for details). Solid line is the reference hydrostatic gradient. Abnormal, high-pressure measurements are enclosed in the polygon.

Consider an active shear zone 10–100 m wide, and a displacement rate of 1–3 mm/yr; these are appropriate parameters for the Castle Mountain fault. The upper and lower bound shear strain rates for this combination of displacement rates and shear-zone widths are: 3.2×10^{-12} s $^{-1} \leq \gamma \leq 9.2 \times 10^{-11}$ s $^{-1}$. If the rate of compaction normal to the shear zone is 10% of γ , then

$$3.2 \times 10^{-14} \text{ s}^{-1} \leq \Gamma \leq 9.2 \times 10^{-13} \text{ s}^{-1},$$

a volumetric strain rate that is orders of magnitude greater than that estimated for regionally distributed shortening strain, and one to two orders of magnitude greater than hydrodynamic forcing by sedimentary compaction.

Poroelastic strain creates pressure pulses ranging from a few tenths to several MPa in com-

pressional and dilatational lobes around the core of a ruptured fault (Scholz, 1990). Poroelastic pressure pulses apparently decay within 0.1–100 yr because fluid diffuses into the surrounding rock and equilibrates pressure between the compressional and dilatational lobes (H. Wang, 1998, personal commun.). This decay time is much shorter than the estimated recurrence interval of $\geq 10^3$ yr for reverse and oblique-slip faults in Cook Inlet anticlines (Haeussler et al., in press).

Glacial Loading. High fluid pressure may be generated in rocks beneath glacial ice sheets where fluid is trapped in low-permeability rock, or in reservoirs surrounded by low-permeability rock (Bahr et al., 1994; Thorpe, 1996). Γ is estimated by substituting the specific weight of ice ($\gamma = 9.0 \times 10^3$ kg m $^{-2}$ s $^{-2}$) for

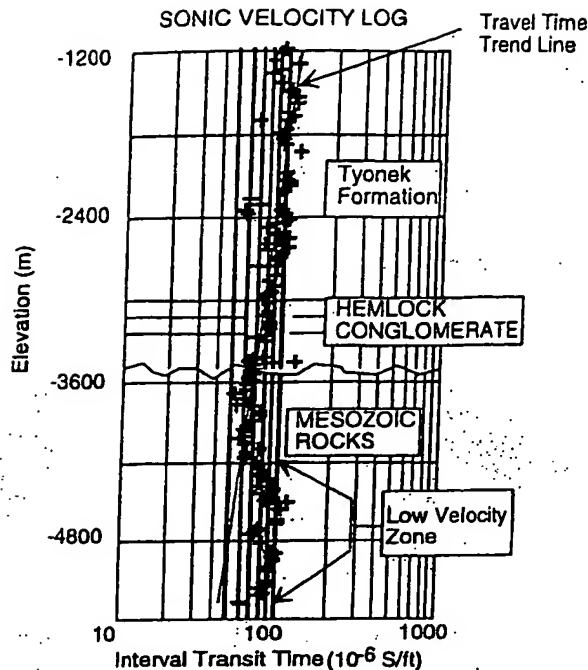


Figure 7. Interval transit time (ITT) in sandstone beds as a function of depth in the SCU-33-33 well, in the Swanson River fold. Each gray cross represents the interval transit time in microseconds per foot of compressional waves in sandstone adjacent to the well bore. Sandstone layers were identified using the spontaneous potential and gamma ray logs following procedures described by Serra (1986). Straight line represents the trend of ITT with depth between 1200 m and 3200 m found by linear regression. Note the high ITT (low sonic velocity) in a bed just above the Tertiary-Mesozoic rock unconformity, and the extensive zone of low velocity below 4000 m. The low compressional wave velocity reflects undercompaction that is presumably caused by high fluid pressure.

that of water-saturated rock and deleting the thermal term in equation 1. Assuming an ice-thickening (accumulation) rate of 10^{-2} m/yr to 10^0 m/yr results in $\Gamma = 1.5 \times 10^{-14} \text{ s}^{-1}$ to $1.5 \times 10^{-12} \text{ s}^{-1}$, comparable to hydrodynamic forcing in fault zones (Table 3). Cook Inlet basin was glaciated during the late Pleistocene as ice lobes advanced into the basin from the Alaska Range and Chugach-Kenai Mountains, but the glaciers retreated from the basin by ≈ 15 k.y. ago (Karlstrom, 1964; Schmoll et al., 1984; Reger, 1983). Consequently, any anomalous fluid pressure generated by ice loading is relic and decaying.

Process Category 2: Hydrocarbon Generation and Alteration

Conversion of solid kerogen and coal to liquid and gaseous hydrocarbons, and thermal alteration of oil to gas, may generate abnormal fluid pressure (Neuzil, 1995; Barker, 1987, 1990; Osborne and Swarbrick, 1997). Middle Jurassic source rocks are overmature in the deeper part of Cook Inlet basin, however, and the low gas to oil ratio in lower Tertiary reservoirs (gas/oil < 1000) suggests that gas production is probably not vigorous at present

(L. Magoon, 1994, and 1998, personal commun.). Thermal alteration of coal beds at temperatures between 70 and 120 °C may liberate methane and CO_2 and generate high fluid pressure (Hunt, 1996). This process could be occurring in Upper Cretaceous and lower Tertiary strata in parts of the basin. Notably, alteration of organic material may also raise the partial pressure of CO_2 and form carboxylic acid, enhancing secondary porosity in previously cemented beds by dissolution of calcite (e.g., Schmidt and McDonald, 1979). Hydrodynamic forcing by conversion of kerogen to hydrocarbons may be on the order of 10^{-14} s^{-1} (Neuzil, 1995), or perhaps greater (e.g., Barker, 1987, 1990).

Process Category 3: Mineral Dehydration During Diagenesis and Metamorphism

Dehydration of hydrous minerals during diagenesis and metamorphism is a potential source of high fluid pressure (Neuzil, 1995; Hunt, 1996; Osborne and Swarbrick, 1997). Liberation of chemically bound water during alteration of smectite to illite is probably not important in Cook Inlet basin given the relatively small volume of illite in the matrix of lower Tertiary and older

and dehydration of the crust and subjacent emplaced by subduction and underplating release fluid to percolate upward beneath basin. Cretaceous marine rocks equivalent to those exhumed in the Chugach-Kenai Mountain accretionary complex were thrust beneath plate margin in Late Cretaceous and early Tertiary time (Moore et al., 1991), and several hundred kilometers of the Yakutat microplate was subducted during Neogene time (Plafker et al., 1993). There is no direct evidence for fluids from speculative source, but the broadly distributed seismicity at depths between 20 and 35 km (Stephens et al., 1995; Ratchovsky et al., 1995) could be triggered by high-pressure fluid release by dynamo-thermal metamorphism. Neuzil (1995) estimated $\Gamma = 10^{-15} \text{ s}^{-1}$ for mineral dehydration during metamorphism, a value that we adopt for comparison with other mechanisms (Table 3).

DISCUSSION

We find that abnormal fluid pressure occurs sporadically in discrete intervals several meters thick in the lower Tertiary rocks, and speculate that high fluid pressure may be even more extensive in older rocks. This latter speculation is based on fluid pressure and sonic log measurements in the Swanson River anticline (Fig. 7; Table 1). There is no compelling evidence, however, for a laterally extensive, high-pressure fluid compartment below 4 km involving Tertiary rocks, nor for a 1-km-thick calcite-cemented sealing layer that cuts across strata and structure at depths between 3 and 4 km as previously proposed (e.g., Hunt, 1990). He-Zhiyong and Franks (1995) reached a similar conclusion based on their analysis of fluid pressure in Cook Inlet basin.

We propose a conceptual model that links fluid migration in Cook Inlet basin to faulting and the development of high fluid pressure in Mesozoic rocks beneath the basin (Fig. 11). This fault-conduit model integrates our diverse geological, petrological, and geochemical data, together with fluid-pressure measurements (Table 1). In this model, Na-Ca-Cl brine is produced in Mesozoic and possibly older basement rocks beneath the basin. Fluid is expelled during faulting, migrates upward through large reverse- and oblique-slip faults, and is injected into the cores of anticlines along cross-faults and through folded bedding (Fig. 11). Mixing of the Na-Ca-Cl brine with Na-HCO₃ fluid precipitates carbonate minerals. Zeolites are precipitated by Na-Ca-Cl fluid reaction with rock in Mesozoic and lower Tertiary strata. Alternating bands of secondary cement reduce permeability normal to bedding and channel fluid along permeable interbeds. Fault permea-

bility is created by fracturing, and enhanced by transport of fluid at high pressure, which increases fracture aperture by reducing effective stress. Conversely, fault permeability decreases as fluid pressure dissipates in the underlying reservoir (Roberts and Nunn, 1996) and fractures become sealed by zeolite and carbonate cement. This fault-conduit model is similar to that proposed by Sibson (1990) for fluid expulsion through reverse faults, and by Roberts and Nunn (1996) for brine and hydrocarbon migration through normal faults.

The fault-conduit migration model (Fig. 11) is based on several lines of evidence, which we discuss in the following sections.

Basin Fluids and Secondary Cement

Processes related to fluid migration must be considered in the context of the tectonic setting and history of Cook Inlet basin. Sedimentation, diagenesis, and tectonics all combined to produce a forearc basin in which two chemically distinct fluids became vertically stratified because the rate of subsidence was roughly equal to the rate of fluvial sedimentation. Na-Ca-Cl brine that originated in marine Mesozoic strata was buried beneath Tertiary stream and flood-plain deposits. Fresh water trapped in the fluvial strata evolved into Na-HCO₃ brine during diagenesis. Migration and mixing of these two fluids were induced by faulting and folding, and ultimately caused formation of the zeolite and carbonate cement that markedly changed the permeability of the lower Tertiary and Mesozoic rocks.

The distributions of zeolite and carbonate veins and cement are critical aspects of the fault-controlled migration model (Fig. 11). Zeolite cement is confined to Mesozoic and Paleocene strata, but carbonate minerals are found in strata ranging from Mesozoic through early Miocene age. Zeolites are produced by reaction of Na-Ca-Cl brine with Mesozoic sandstone and siltstone. Migration of the Na-Ca-Cl brine into overlying Tertiary rocks proceeds by upward flow of fluid along faults, and lateral spreading of the fluid away from fault exit points into the Tertiary strata (Fig. 11). This migration process forms zeolite and carbonate mineral veins in faults, and precipitates secondary cement in the folded Tertiary rocks. The abundant secondary calcite in conglomerate and coarse sandstone beds presumably reflects mineral precipitation by transport-limited chemical reactions (Fig. 10), where solutes are carried to reaction sites by advection (Phillips, 1991). Initially, the rate of secondary cementing is presumably greater in permeable sandstone and conglomerate beds where fluid flux is concentrated, and less in interbeds of lower permeability siltstone and shale. This process ultimately reduces both the original variation in permeability

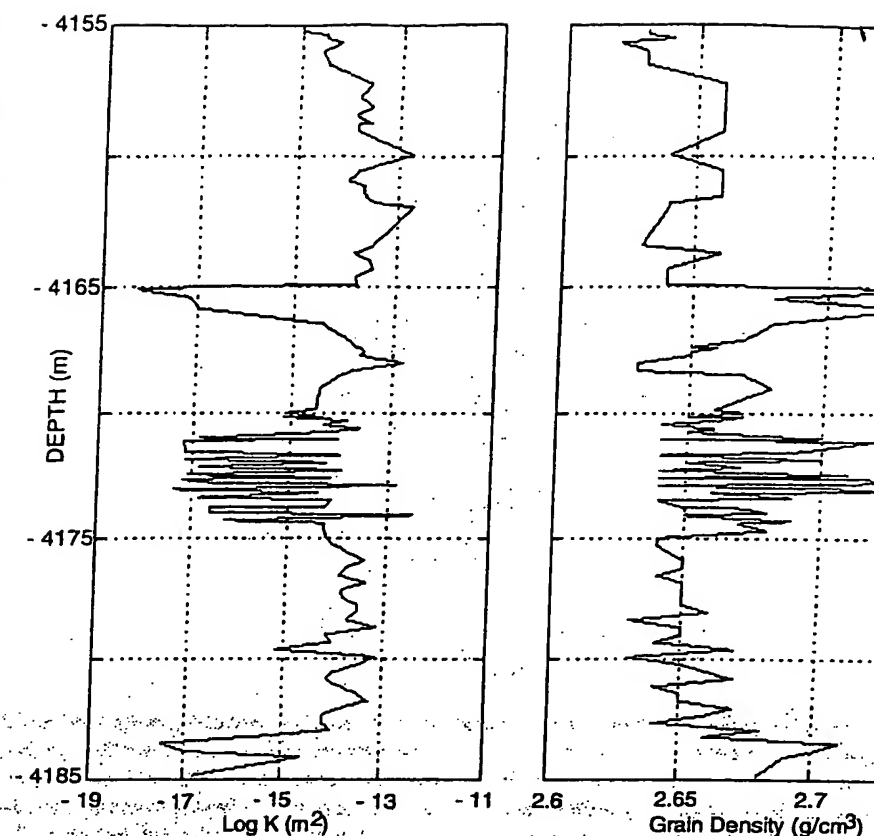


Figure 8. (A) Permeability versus depth for core plugs in a 30-m-thick interval in the Formation, Sunfish #3 well, North Cook Inlet anticline. Note that permeability varies with depth and sample grain density. High grain density is caused by carbonate cement plugs pore space and reduces permeability. 1 mD = $1 \times 10^{-15} \text{ m}^2$.

between adjacent beds, and the mean permeability of the stratigraphic interval (Fig. 8; Phillips, 1991). These cemented intervals are aquitards to fluid flow across bedding, but channel flow through permeable interbeds (Fig. 11).

Geochemical modeling and oxygen isotope compositions of calcite provide additional evidence for the migration of Na-Ca-Cl fluid into lower Tertiary rocks. Calcite cement and vein minerals in lower Tertiary strata developed both by diagenetic reactions between Na-HCO₃ brine and rock grains, and by mixing of this brine with migrated Na-Ca-Cl brine (Fig. 10). Of 10 calcite

cement samples collected from lower Tertiary strata, 6 are relatively light in $\delta^{18}\text{O}$ (Fig. 9) indicating that calcite was probably precipitated by reaction between Na-HCO₃ fluid and rock, presumably during burial diagenesis. The remaining samples of cement have intermediate $\delta^{18}\text{O}$, indicating that this calcite precipitated by mixing of the Na-HCO₃ and migrated Na-Ca-Cl fluid. This migration model is also supported by the isotopic composition of calcite veins in faults, most of which plot along a $\delta^{18}\text{O}$ trend indicative of fluid migration (Fig. 9).

TABLE 2. COMPOSITION OF SUBSURFACE WATER FOR GEOCHEMICAL MODELING

Component	Tertiary fluid source (mg/kg)	Mesozoic fluid source (mg/kg)
	Evolved meteoric water	Evolved sea water
Total dissolved solids	3755	19725
Cl	648 charge balance	11 989 charge balance
HCO ₃	1830	28 calcite saturation
Ca	0.6 calcite saturation	2809
Na	1149	4603
K	2 K-feldspar saturation	53 K-feldspar saturation
Fe	0.04 siderite saturation	21 siderite saturation
Mg	0.01 chlorite saturation	1 chlorite saturation
Al	1 kaolinite saturation	0.1 illite saturation
SiO ₂	35 quartz saturation	31 quartz saturation

The importance of faulting in fluid migration is evidenced by the widespread occurrence of zeolite and carbonate veins in reverse- and strike-slip faults (e.g., Fig. 5). The link between faulting and fluid flow suggests that those processes that create high fluid pressure in the Mesozoic basement are most important on a basinwide scale. Volumetric strain caused by tectonic shortening, and particularly by shearing and compaction in fault zones, is presumably most effective in the Mesozoic and older rocks (Table 3). Deformation may be augmented by metamorphism and mineral dehydration in the middle crust and below, and by thermal alteration of organic-rich rock and hydrocarbons. This latter process was more vigorous in the past than at present, given the hydrocarbon maturation history proposed by Magoon (1994, and 1998, personal commun.). Sedimentary loading and compaction in synclines may also generate high fluid pressure, perhaps driving fluid laterally into fault zones or upward along bedding in anticlines (He-Zhiyong and Franks, 1995). Thermal alteration of coal beds in Upper Cretaceous and lower Tertiary strata could also create high fluid pressure, but this process cannot be the driving mechanism for flow of Na-Ca-Cl brine out of older marine strata.

The fault-controlled fluid-migration model provides a rationale for the heterogeneous distribution of fluid pressure in some Cook Inlet anticlines. The pressure, spatial dimension, and lifetime of a plume of injected fluid depends on the pressure of the source region relative to that at the fault exit point, the fluid flux, duration of flow, and the permeability and storativity of the rocks into which the fluid is injected (Roberts and Nunn, 1996). Generation of long-lasting pressure anomalies is facilitated by catastrophic rupturing of the fault conduit, which greatly enhances permeability, and therefore fluid flux. The duration of flow is controlled by the rate of pressure depletion in the source zone, the sensitivity of fracture permeability to increases in effective normal stress (Roberts and Nunn, 1996), and porosity reduction by mineral precipitation. The time scale for catastrophic rupturing is the recurrence interval of large earthquakes on active faults, which is probably $\geq 10^3$ yr for the large reverse and oblique-slip faults coring Cook Inlet anticlines (Haeussler et al., in press). Fluid may also seep through fault conduits if fracturing occurs by fault creep, as the result of static strain changes induced in the basin by great subduction-zone earthquakes like the $M = 9.2$ event of 1964, or by dynamic stresses induced as seismic waves

propagate through the basin. Great subduction-zone earthquakes occur at ~ 700 yr intervals (Combellick, 1991). Smaller earthquakes that originate in the subduction zone or lower crust beneath Cook Inlet (Fig. 1) are felt on a weekly to monthly basis.

Migration History and Cenozoic Tectonics

Fluid migration in Cook Inlet basin occurred in two primary phases. Hydrocarbons that migrated into traps prior to the onset of Eocene deformation were presumably lost during erosion prior to deposition of the Hemlock and correlative conglomerates in late Oligocene time, according to Magoon (1994). Migration of Na-Ca-Cl brine out of Mesozoic beds presumably initiated zeolite and carbonate deposition in Mesozoic and lower Tertiary rocks during this early period of deformation and fluid migration. The second phase of oil and brine migration followed deposition of the lower and middle Miocene Tyonek Formation, and was accompanied by growth of fault-propagation anticlines that form structural traps throughout the basin (Figs. 2 and 4; Magoon, 1994). Reverse- and oblique-slip faults provided the primary conduits for migration of Na-Ca-Cl brine and hydrocarbons into the cores of these anticlines, as previously discussed. Here we note that siltstone and clay-rich layers at the base of coal beds are usually assumed to be the hydrocarbon trap rock (Magoon, 1994), but in our opinion, secondary cement is probably an important, yet overlooked, factor in permeability reduction and trap formation within Cook Inlet anticlines.

We have studied only a few of the more than 24 faults and anticlines located within Cook Inlet

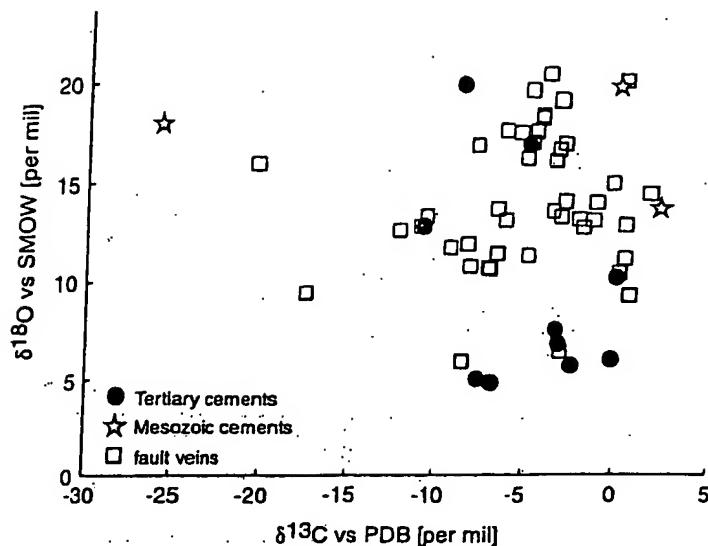


Figure 9. Carbon and Oxygen isotopic measurements for calcite in fault veins and cement Mesozoic and Tertiary rocks. PDB—Peedee belemnite; SMOW—standard mean ocean water. See text for discussion.

basin (Fig. 2). Some of these folds are known to contain abnormal fluid pressure (Table 1); others apparently do not (e.g., Middle Ground Shoal anticline). There are, however, few pressure measurements in pre-Tertiary rocks (Table 1). The fault-controlled fluid migration model (Fig. 11) provides a conceptual framework that is amenable to testing and refinement as exploration and drilling continues in the future. The model has the potential to guide hydrocarbon exploration and development strategies, as well as provide insight into possible links between tectonic activity, fluid migration, and fluid-pressure distribution. This latter topic is of considerable importance for understanding fault stability and potential for earthquake generation. Careful study of the Quaternary geology is required to determine which folds are active, and if there is a correlation between subsurface fluid pressure and active faulting.

CONCLUSIONS

Faulting controls fluid migration in Cook Inlet basin. Fluid is expelled from Mesozoic source rocks in the basement, flows upward through faults, and is injected into Tertiary strata in the cores of anticlines. Fluid migration is presumably episodic, with the greatest fluid flux following catastrophic fault rupturing and earthquake generation, which may occur every several thousand years in actively growing folds. Migration may also occur by fluid seepage where fault permeability is maintained by creep or stress transients. Fault permeability is reduced or sealed by precipitation of zeolite and carbonate veins.

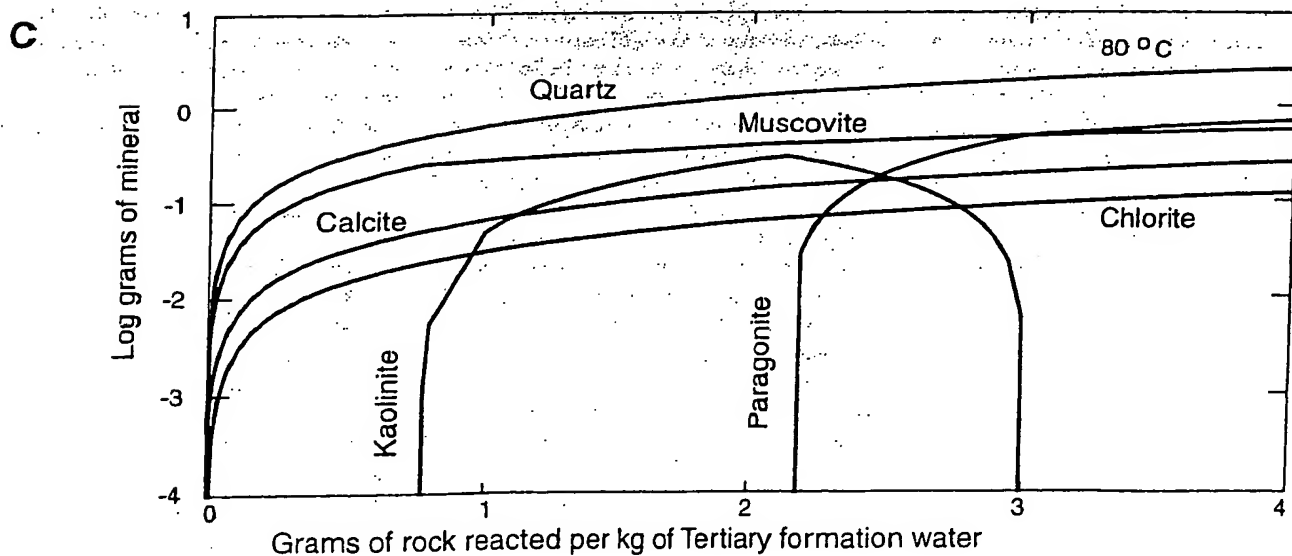
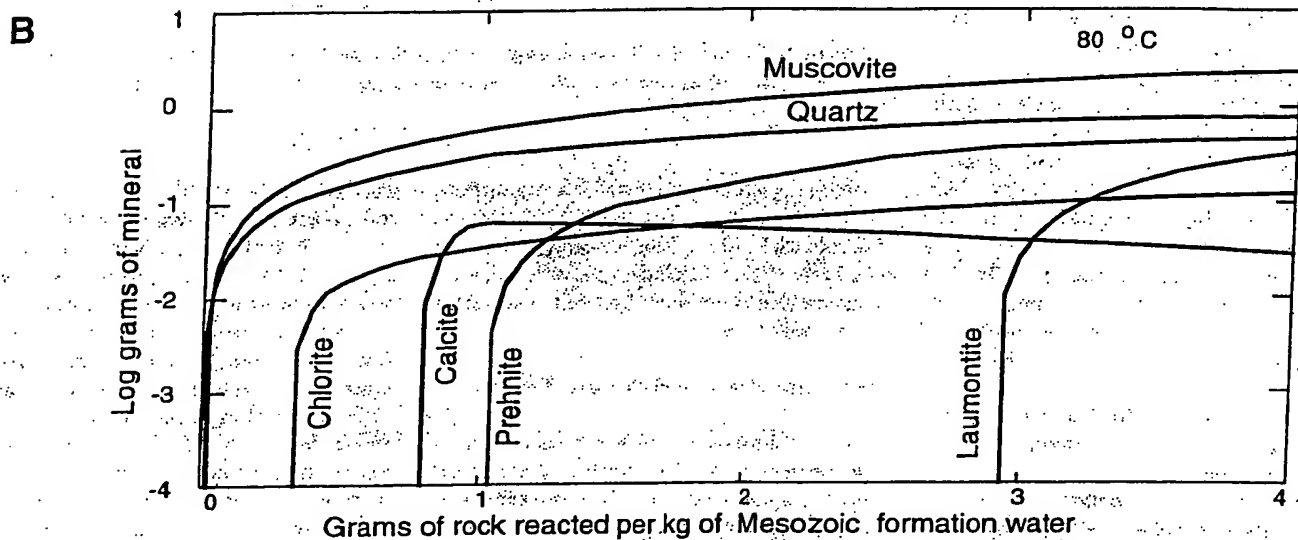
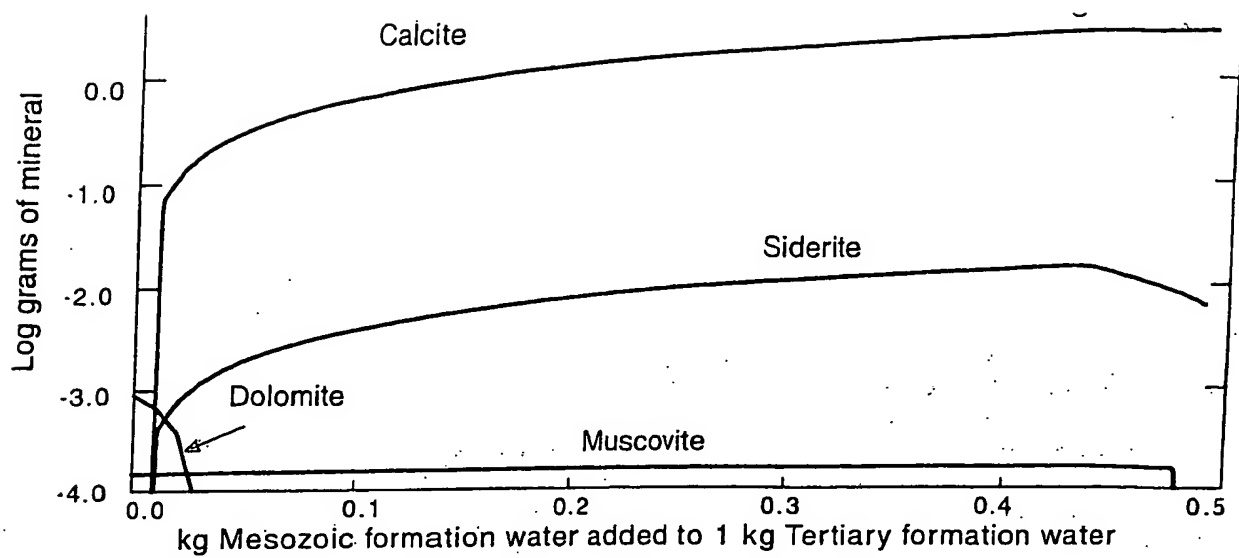


Figure 10. Geochemical simulations showing mineral products precipitated during (A) Na-Ca-Cl and Na-HCO₃ brine-mixing reactions; (B) Na-Ca-Cl brine-rock reactions; and (C) Na-HCO₃ brine-rock reactions.

Hydrodynamic process	Hydrodynamic forcing (1/s)	Minimum reservoir length (L) (Permeability $k = 1 \text{ E}^{-18} \text{ m}^2$)	Comments
Sedimentary compaction	$\leq 4 \times 10^{-15}$	$\geq 25 \text{ km}$	Focused into synclines
Distributed tectonic shortening	$\approx 3 \times 10^{-17}$	$> 100 \text{ km}$	Not reasonable reservoir dimension
Fault creep and tectonic compaction	3×10^{-14} to 9×10^{-13}	$< 1 \text{ km}$	Shearing rate of 1–3 mm/yr
Fault rupture (Poroeastic)	Instantaneous pulse of 1–10 MPa	Affects region of several kilometers surrounding fault	Pressure pulse decays in periods of 10 to 1000 yr
Glacial loading	1.5×10^{-14} to 1.5×10^{-12}	$< 1 \text{ km}$	Pre-Holocene loading
Hydrocarbon generation and/or alteration	$\geq 1 \times 10^{-14}$	$\leq 2 \text{ km}$	Thermogenic and biogenic alteration of organic matter and hydrocarbons
Prograde metamorphism	$\leq 1 \times 10^{-15}$	$\geq 20 \text{ km}$	Middle crust and deeper source (?)

Note: Increase or decrease reservoir length by a factor of 10 for each decade increase or decrease in permeability.

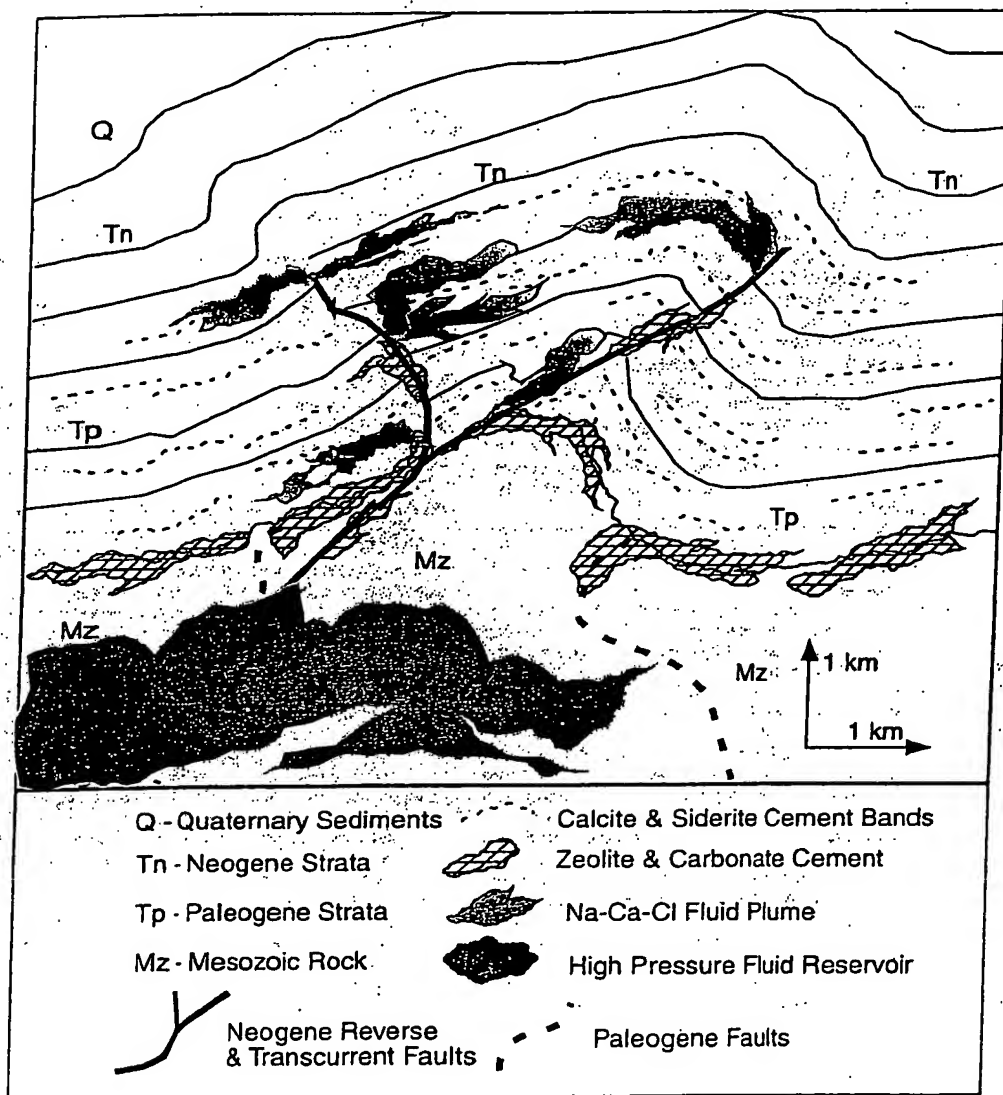


Figure 11. Conceptual model of fluid migration in a fault-propagation fold. High-pressure fluid originates in the Mesozoic or older rocks beneath the basin, migrates upward along faults, and is injected as plumes of Na-Ca-Cl brine in lower Tertiary rocks. Zeolite cement and veins are precipitated by reaction of Na-Ca-Cl brine with sedimentary rock grains. Calcite and other carbonates are deposited where Na-Ca-Cl brine reacts during mixing with Na-HCO₃ fluid in Tertiary strata. Some carbonate cement is also precipitated by reaction of Na-HCO₃ brine and rock fragments during burial diagenesis. See text for detailed discussion of the migration model.

The basin contains two different pore fluid. Na-Ca-Cl brine reacts with sedimentary rock fragments to form secondary zeolite cement in Mesozoic and Paleocene rocks and veins in faults. Na-HCO₃ connate fluid in Tertiary strata reacts with rock, and mixes with migrate Na-Ca-Cl brine to precipitate carbonate mineral in sedimentary pore space and fault veins. Fluctuations in the partial pressure of CO₂ also result in precipitation of carbonate cement and veins but this process is inefficient relative to fluid-rock and fluid-mixing reactions, which require much less volume of fluid per gram of calcite produced.

High fluid pressure may originate by a variety of mechanisms acting either alone or together at different times and locations within the basin. Generation of high fluid pressure in the basement is presumably important given the evidence for fault-controlled migration of brines and hydrocarbons in anticlines. Volumetric strain caused by tectonic shortening and shearing, and dynamothermal metamorphism in the middle crust are perhaps most important in basement rocks. Other, alternative mechanisms include alteration of organic-rich rocks and hydrocarbons, sedimentary loading and compaction, and possibly relic pressure generated by glacial loading during late Pleistocene time.

ACKNOWLEDGMENTS

This work was supported by National Science Foundation grant EAR-9316347 awarded to Bruhn and Parry, and a grant from the National Earthquake Hazards Program awarded to Bruhn. ARCO Alaska, Inc., provided access to seismic reflection profiles, core samples, and thin sections. We specifically thank David Bannon of ARCO, Alaska, Inc., for his help. John Reeder of the Alaska Division of Geological and Geophysical Surveys provided access to cores and thin sections on file in the State of Alaska core repository in Eagle River, Alaska. S. Franks of ARCO provided information on the chemistry of fluids collected from wells in Cook Inlet basin, and his discussions were very helpful. We also acknowledge discussions with D. Seamount of UN-

OCAL, and P. J. Haeussler and T. R. Pratt of the U.S. Geological Survey. Collaboration with P. J. Haeussler in the field during part of this study was particularly useful. Comments by L. Magoon and D. Seamont on a draft of the manuscript were also appreciated.

REFERENCES CITED

- Alaska Oil and Gas Conservation Commission (AOGCC), 1994, 1994 Statistical report, 230 p.
- Bahr, J. M., Moline, G. R., and Nadon, G. C., 1994, Anomalous pressures in the deep Michigan basin, in Ortoleva, P., ed., *Basin compartments and seals: American Association of Petroleum Geologists Memoir 61*, p. 153-165.
- Barker, C., 1987, Development of abnormal and subnormal pressures in reservoirs containing bacterially generated gas: *American Association of Petroleum Geologists Bulletin*, v. 71, p. 1404-1413.
- Barker, C., 1990, Calculated volume and pressure changes during thermal cracking of oil to gas in reservoirs: *American Association of Petroleum Geologists Bulletin*, v. 74, p. 1254-1261.
- Barnes, F., and Payne, T. G., 1956, The Wishbone Hill Mining district, Matanuska coal field, Alaska: *U.S. Geological Survey Bulletin 1016*, 68 p.
- Blanpied, M. L., Lockner, D. A., and Byerlee, J. D., 1992, An earthquake mechanism based on rapid sealing of faults: *Nature*, v. 358, p. 574-576.
- Boss, R. F., Lennon, R. B., and Wilson, B. W., 1976, Middle Ground Shoal oil field, Alaska, in Braunstein, J., ed., *North American oil and gas fields: American Association of Petroleum Geologists Memoir 24*, p. 1-22.
- Bredehoeft, J. D., and Hanshaw, B. B., 1968, On the maintenance of anomalous fluid pressures: I. Thick sedimentary sequences: *Geological Society of America Bulletin*, v. 79, p. 1097-1106.
- Bruhn, R. L., and Pavlis, T. L., 1981, Late Cenozoic deformation in the Matanuska Valley, Alaska: Three-dimensional strain in a forearc region: *Geological Society of America Bulletin*, v. 92, p. 282-293.
- Byerlee, J. D., 1993, Model for episodic flow of high pressure H₂O in fault zones before earthquakes: *Geology*, v. 21, p. 289-304.
- Calderwood, K. W., and Fackler, W. C., 1972, Proposed stratigraphic nomenclature for Kenai Group, Cook Inlet basin, Alaska: *American Association of Petroleum Geologists Bulletin*, v. 56, p. 739-754.
- Clardy, B. I., 1974, Origin of the lower and middle Tertiary Wishbone and Tsadaka Formations, Matanuska valley, Alaska [M.S. thesis]: Fairbanks, University of Alaska, 74 p.
- Claypool, G. E., Threlkeld, C. N., and Magoon, L. B., 1980, Biogenic and thermogenic origins of natural gas in Cook Inlet basin, Alaska: *American Association of Petroleum Geologists Bulletin*, v. 64, p. 1131-1139.
- Combellick, R. A., 1991, Paleoseismicity of the Cook Inlet region, Alaska: Evidence from peat stratigraphy in Turnagain and Knik Arms: *Alaska Division of Geological and Geophysical Surveys Professional Report 112*, 52 p.
- Deming, D., 1994, Factors necessary to define a pressure seal: *American Association of Petroleum Geologists Bulletin*, v. 78, p. 1005-1009.
- Detterman, R. L., Plafker, G., Hudson, T., Tysdal, R. G., and Pavoni, N., 1974, Surface geology and Holocene breaks along the Susitna segment of the Castle Mountain fault, Alaska: *U.S. Geological Survey Miscellaneous Field Studies Map MF-618*, 1 sheet, scale 1:24,000.
- Dickinson, W. R., and Seeley, R. M., 1979, Structure and stratigraphy of forearc regions: *American Association of Petroleum Geologists Bulletin*, v. 63, p. 2-31.
- Fisher, M. A., and Magoon, L. B., 1978, Geologic framework of lower Cook Inlet, Alaska: *American Association of Petroleum Geologists Bulletin*, v. 62, p. 373-402.
- Franks, S. G., and He-Zhiyong, 1995, Subsurface waters, upper Cook Inlet, Alaska, Part I: Geochemistry: *American Association of Petroleum Geologists and Society of Economic Paleontologists and Mineralogists Annual Meeting Abstracts*, v. 4, p. 30.
- Grantz, A., 1966, Strike-slip faults in Alaska: *U.S. Geological Survey Open-File Report 66-53*, 92 p.
- Haeussler, P. H., Bruhn, R. L., and Pratt, T. L., Pliocene or Quaternary deformation in upper Cook Inlet, Alaska (in press).
- Hartman, D. C., Pessel, G. H., and McGee, D. L., 1972, Preliminary report on stratigraphy of Kenai Group, upper Cook Inlet, Alaska: *Alaska Division of Geological Surveys Special Report 54*, 7 maps, scale 1:500,000.
- Hayes, J. B., 1979, Sandstone diagenesis—The hole truth, in Scholle, P. A., and Schluger, P. R., eds., *Aspects of diagenesis: Society of Economic Paleontologists and Mineralogists Special Publication 26*, p. 127-140.
- He-Zhiyong, and Franks, S. G., 1995, Subsurface water, upper Cook Inlet, Alaska; Part II, Hydrodynamics: *American Association of Petroleum Geologists and SEPM Annual Meeting Abstracts*, v. 4, p. 41.
- Hunt, J. M., 1990, Generation and migration of petroleum from abnormally pressured fluid compartments: *American Association of Petroleum Geologists Bulletin*, v. 74, p. 1-12.
- Hunt, J. M., 1996, *Petroleum geochemistry and geology*: New York, W. H. Freeman Co., 743 p.
- Karlstrom, T. N. V., 1964, Quaternary geology of the Kenai lowland and glacial history of the Cook Inlet region, Alaska: *U.S. Geological Survey Professional Paper 443*, 69 p.
- Kirschner, C. E., and Lyon, C. A., 1973, Stratigraphic and tectonic development of Cook Inlet petroleum province, in Pitcher, M. G., ed., *Arctic geology: American Association of Petroleum Geologists Memoir 19*, p. 396-407.
- Little, T. A., 1991, Development of wrench folds along the Border Ranges fault system, southern Alaska, USA: *Journal of Structural Geology*, v. 14, p. 343-359.
- Lyle, W. M., and Morehouse, J. A., 1977, Physical parameters of potential petroleum reservoir and source rocks in the Kamishak-Iniskin-Tuxedni region, lower Cook Inlet, Alaska: *Alaska Division of Geological and Geophysical Surveys Open-File Report 104*, 89 p.
- Magoon, L. B., 1994, Tuxedni-Hemlock petroleum system in Cook Inlet, Alaska, in Magoon, L. B., and Dow, W. G., eds., *The petroleum system from source to trap: American Association of Petroleum Geologists Memoir 60*, p. 359-370.
- Magoon, L. B., and Claypool, G. E., 1981, Petroleum geology of Cook Inlet basin, Alaska—an exploration model: *American Association of Petroleum Geologists Bulletin*, v. 65, p. 1043-1061.
- Magoon, L. B., Greisbach, F. R., and Egbert, R. M., 1980, Non-marine Upper Cretaceous rocks, Cook Inlet, Alaska: *American Association of Petroleum Geologists Bulletin*, v. 64, p. 1259-1266.
- McGee, D. L., 1977, Salinity study, Cook Inlet basin, Alaska: *Alaska Division of Geological and Geophysical Surveys Geologic Report 54*, 6 p.
- Moore, J. C., Diebold, J., Fisher, M. A., Sample, J., Brocher, T., Talwani, M., Ewing, J., von Heune, R., Rowe, C., Stone, D., Stevens, C., and Sawyer, D., 1991, EDGE deep seismic reflection transect of the eastern Aleutian arc-trench layered lower crust reveals underplating and continental growth: *Geology*, v. 19, p. 420-424.
- Neuzil, C. E., 1995, Abnormal pressures as hydrodynamic phenomena: *American Journal of Science*, v. 295, p. 742-786.
- Ortoleva, P., Al-Shaib, Z., and Puckette, J., 1995, Genesis and dynamics of basin compartments and seals: *American Journal of Science*, v. 295, p. 345-427.
- Osborne, M. J., and Swarbrick, R. E., 1997, Mechanisms for generating overpressure in sedimentary basins: A reevaluation: *American Association of Petroleum Geologists Bulletin*, v. 81, p. 1023-1041.
- Page, R. A., Biswas, N. N., Lahr, J. C., and Pulpan, H., 1991, Seismicity of continental Alaska, in Slemmons, D. B., Engdahl, E. R., Zoback, M. D., and Blackwell, D. D., eds., *Neotectonics of North America: Geological Society of America, Decade of North American Geology Map Volume*, p. 47-68.
- Pavlis, T. L., 1982, Origin and age of the Border Ranges fault of southern Alaska and its bearing on the late Mesozoic tectonic evolution of Alaska: *Journal of Geophysical Research*, v. 87, p. 343-368.
- Phillips, O. M., 1991, *Flow and reactions in* Cambridge, Cambridge University Press.
- Plafker, G., Moore, J. C., and Winkler, G. R., eds., 1980, The southern Alaska margin, in Plafker, G. R., Moore, J. C., and Winkler, G. R., eds., *Geology of Alaska: Geological Society of America, Geology of Alaska*, v. G-1, p. 389-449.
- Powley, D. E., 1990, Pressures and hydrogeological basins: *Earth-Science Reviews*, v. 29, p. 1-17.
- Ratchkovsky, N. A., Pujol, J., and Biswas, N. N., 1990, Initiation of shallow earthquakes in southern Alaska: *Hypocenter Determination method: Bulletin of the Geological Society of America*, v. 87, p. 6-17.
- Reed, M. H., 1982, Calculation of multicomponent equilibria and reaction processes in systems: *Cosmochimica Acta*, v. 46, p. 513-528.
- Reger, R. D., 1983, Upper Cook Inlet, Matanuska Valley, in Pewe, T. L., and Rej, Guidebook to permafrost and Quaternary the Richardson and Glenn Highways betw and Anchorage: *Alaska Division of Natural Division of Geological and Geophysical Surveys*, p. 185-263.
- Roberts, S. J., and Nunn, J. A., 1996, Expulsion of pressured fluids along faults: *Journal of Geophysical Research*, v. 101, p. 28,231-28,252.
- Schmidt, V., and McDonald, D. A., 1979, The role of porosity in the course of sandstone diagenesis: *Journal of Geophysical Research*, v. 84, p. 175-207.
- Schmoll, H. R., Yellich, L. A., Gardner, C. A., and 1984, Guide to surficial geology and glacial in the upper Cook Inlet basin: Anchorage, Alaska: *Alaska Division of Geological and Geophysical Surveys*, 89 p.
- Schultz, C. H., 1990, *The mechanics of faulting and earthquakes*: Cambridge, Cambridge University Press.
- Serra, O., 1986, Fundamentals of well-log interpretation—The interpretation of logging data: Elsevier Science Publishers, *Developments in Petroleum Science*, no. 15B, 689 p.
- Sibson, R. H., 1990, Conditions for fault-valve behavior: *Journal of Geophysical Research*, v. 95, p. 15,177-15,197.
- Silberling, N. J., Jones, D. L., Coney, P. J., Berg, P. L., Plafker, G., Jones, D. L., and Berg, H. C., eds., 1994, *Geological Society of America, Geological Society of America, G-1, plate 3*.
- Sleep, N., and Blanpied, M., 1992, Creep, compaction, and weak rheology of major faults: *Nature*, v. 359, p. 618-622.
- Stamatokos, J. A., Kodama, K. P., and Pavlis, T. L., 1989, Paleomagnetism of Eocene plutonic rocks, Matanuska Valley, Alaska: *Geology*, v. 16, p. 618-622.
- Stamatokos, J. A., Kodama, K. P., Vittorino, L. F., and T. L., 1989, Paleomagnetism of Cretaceous arcine sedimentary rocks across the Castle Mountain south-central Alaska: *American Geophysical Union Monograph* 50, p. 151-177.
- Stephens, C. D., Page, R. A., Lahr, J. C., and Fogelma, 1995, Crustal seismicity in the Anchorage area: *Alaska: Geological Society of America Abstracts*, v. 27, no. 5, p. 78-79.
- Thorson, R. M., 1996, Earthquake recurrence and glacial in western Washington: *Geological Society of America Bulletin*, v. 108, p. 1182-1196.

MANUSCRIPT RECEIVED BY THE SOCIETY JUNE 22, 1998
REVISED MANUSCRIPT RECEIVED MARCH 12, 1999
MANUSCRIPT ACCEPTED MAY 12, 1999